11374–11386 *Nucleic Acids Research, 2022, Vol. 50, No. 19* *Published online 27 October 2022*
https://doi.org/10.1093/nar/gkac846

Expansion of the genetic code through reassignment of redundant sense codons using fully modified tRNA

Clinton A.L. McFeely[1,2], Kara K. Dods[1,2], Shivam S. Patel[1] and Matthew C.T. Hartman[1,2,*]

[1]Department of Chemistry, Virginia Commonwealth University, Richmond, VA 23220, USA and [2]Massey Cancer Center, Virginia Commonwealth University, Richmond, VA 23220, USA

Received March 31, 2022; Revised September 09, 2022; Editorial Decision September 12, 2022; Accepted September 23, 2022

ABSTRACT

Breaking codon degeneracy for the introduction of non-canonical amino acids offers many opportunities in synthetic biology. Yet, despite the existence of 64 codons, the code has only been expanded to 25 amino acids *in vitro*. A limiting factor could be the over-reliance on synthetic tRNAs which lack the post-transcriptional modifications that improve translational fidelity. To determine whether modified, wild-type tRNA could improve sense codon reassignment, we developed a new fluorous method for tRNA capture and applied it to the isolation of roughly half of the *Escherichia coli* tRNA isoacceptors. We then performed codon competition experiments between the five captured wild-type leucyl-tRNAs and their synthetic counterparts, revealing a strong preference for wild-type tRNA in an *in vitro* translation system. Finally, we compared the ability of wild-type and synthetic leucyl-tRNA to break the degeneracy of the leucine codon box, showing that only captured wild-type tRNAs are discriminated with enough fidelity to accurately split the leucine codon box for the encoding of three separate amino acids. Wild-type tRNAs are therefore enabling reagents for maximizing the reassignment potential of the genetic code.

GRAPHICAL ABSTRACT

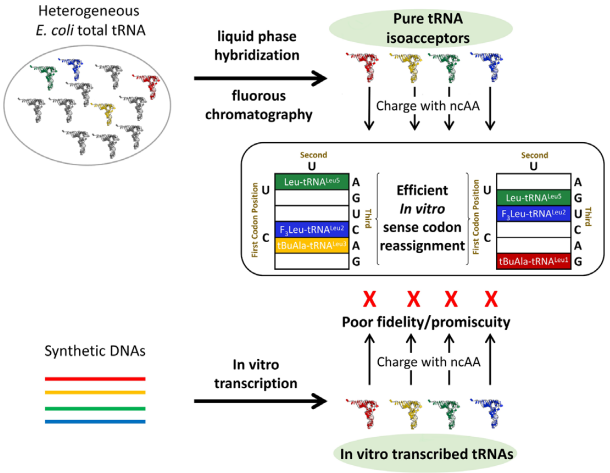

INTRODUCTION

Genetic code expansion (GCE) technologies aim to meet rising demand for designer peptides and proteins with site-specific chemical modifications. Proteins made via GCE usually feature one to two non-canonical amino acids (ncAAs), often introduced through repurposed stop codons or quadruplet codons, resulting in new conjugation handles, altered residue reactivity and fluorescent tracers, to name but a few customizations (1–3). GCE technologies paired with peptide discovery platforms could lead to more clinically suitable drug leads by generating diverse libraries with improved pharmacological features, such as lowered molecular weight, enhanced rigidity, cyclization and reduced number of hydrogen bonds and acceptors (4–8).

One central goal in GCE is to increase the total number of usable amino acid monomers beyond the canonical 20. In this regard, different GCE techniques have various degrees of promise. Stop codon suppression, for example, is limited by the existence of just the three stop codons: amber, opal and ochre, and the competing presence of release factors, resulting in the addition of no more than three ncAAs (9,10). Translation of quadruplet codons has seen impres-

*To whom correspondence should be addressed. Email: mchartman@vcu.edu

sive and rapid improvement, permitting as many as four expansion sites in a protein, yet the efficiency of this technique remains low (11–13). Novel, unnatural nucleotides have been designed that are capable of selective base pairing and are compatible with various types of cellular biomachinery, allowing their incorporation into biomolecules such as mRNA and tRNA, yet it remains unclear how many unnatural base pairs may be supported together for GCE (14,15).

Sense codon reassignment (SCR) focuses on breaking the degeneracy of the genetic code to introduce ncAAs. Amongst the 61 naturally occurring sense codons, there exists a great deal of redundancy, as groups of two, three, four and even six codons are synonymously read by families of tRNA isoacceptors. Such degenerate codon boxes can be reassigned, maintaining one codon for the naturally encoded amino acid, and reassigning the others to ncAAs. SCR is a highly promising GCE technique, especially in the field of cell-free *in vitro* translation where translation components may be easily replaced or omitted (16–21). SCR *in vitro* has already achieved an expansion of the code up to 25 monomers, making it one of the best examples of GCE described to date (22,23). Additionally, redundant sense codons have even been reduced or completely eliminated from bacterial genomes without causing deleterious effects to the host organism, signaling *in vivo* potential as well (24–27). Despite these efforts, the magnitude of genetic code expansion is still small relative to the number of codons, and these efforts are plagued with challenges due to misincorporations and unexpected codon reading patterns (28).

Maximizing the number of ncAAs added to a codon box requires a high degree of discrimination between tRNA isoacceptors in order to maintain fidelity. Such discrimination is a complex process, driven by numerous contact points between the ribosomal subunits, various domains of tRNA and the ternary complex formed between elongation factor thermally unstable (EF-Tu), aminoacylated tRNA (AA-tRNA) and GTP (29–32). tRNA post-transcriptional modifications (PTMs) are known to play an important role in maintaining codon readthrough fidelity (33–36). Unmodified synthetic tRNA (t7tRNA) was shown to enter the ribosomal decoding center with much greater conformational freedom than modified, wild-type tRNA (wt tRNA), creating an entropic penalty to restrain the tRNA to the correct conformation prior to codon anticodon base pairing (35). PTMs are also known to help maintain the correct codon reading frame, assist in tRNA translocation from the A to P site of the ribosome and alter the codons that are read by the modified tRNA (34,37–39). Furthermore, PTMs can serve as important recognition features for aminoacylation by aminoacyl-tRNA synthetases (aaRSs) (40–42).

Despite the known importance of PTMs, t7tRNA and engineered synthetic tRNA lacking PTMs are most commonly used for *in vitro* SCR, often at elevated concentrations (22). We hypothesized that fully modified wt tRNAs would prove to be better substrates than t7tRNA, permitting more complex SCR schemes, such as the encoding of multiple ncAAs within a single codon box. This, however, required a reliable tRNA capture method for obtaining wt tRNA. While a handful of such methods have been reported, most use solid-phase immobilization of oligonucleotide probes, suffer from slow reaction kinetics, have limited proven applicability or have insufficient yields for our purposes (43–45). Here we describe a new, scalable method for the isolation of modified wt tRNA, based on liquid phase hybridization and fluorous chromatography. We then designed a direct codon competition assay that puts wt tRNAs head-to-head against their t7tRNA counterparts for readthrough of a cognate codon. Finally, we executed two different SCR schemes within the 6-fold degenerate leucine codon box.

MATERIALS AND METHODS

Reagents

Escherichia coli total RNA was purchased from Roche. Fluorous columns, phosphoramidite reagents and fluorous CPG resin were acquired from BioSearch Technologies. The d3, d7 and d17 leucine isotopes were acquired from Sigma-Aldrich and the d10 leucine isotope was acquired from CDN Isotopes.

Equipment

Urea–polyacrylamide gel electrophoresis (PAGE) gels were imaged on a ChemiDoc MP Imaging System (Bio-Rad). Sample absorbance was measured on a NanoDrop ND-1000 SpectroPhotometer. Mass spectrometry experiments were performed on a Voyager-DE Pro BioSpectrometry Workstation (Applied Biosystems) under reflectron positive mode.

Oligonucleotide synthesis

Deoxyribose oligonucleotide probes were synthesized on a MerMade 4 (BioSearch Technologies) using standard phosphoramidite chemistry, starting from a 3′-fluorous modifier (BioSearch Technologies). Oligos were cleaved from the resin supports by adding 500 μl of 1:1 concentrated ammonium hydroxide and 40% methylamine followed by incubation at 55°C for 15 min. Cleaved oligos were extracted into 1-butanol via centrifugation at 4°C, followed by ethanol precipitation. Finally, the oligo pellets were resuspended in water and stored at –20°C. Purity of the oligos was examined through electrophoresis or matrix-assisted laser desorption/ionization mass spectrometry (MALDI-MS) and subjected to further purification via denaturing PAGE (12%) on a case by case basis, when truncated oligos were observed.

Hybridization

Lyophilized total RNA from *E. coli* MRE 600 (Roche) was dissolved in water to 100 mg/ml, stored at –80°C and used as the tRNA stock for all capture experiments. Low-scale hybridization mixtures were prepared by mixing 20 μl of 5× hybridization buffer (1 M KCl, 0.5 mM EDTA, 250 mM HEPES, pH 7.5) with fluorous-tagged oligo (100 μM), adding 20 μl of total tRNA (100 mg/ml), and diluting with water to 100 μl. For higher scale captures, each ingredient within the mix was scaled up equally, frequently by 100–200×. The amount of oligo used was based on the predicted abundance of the target isoacceptor (46). The mixture was

then fully denatured on a thermocycler by heating at 90°C for 1 min, followed by 10 min of controlled heating at 3°C below the melting temperature (T_m).

Fluorous affinity chromatography

For ease of use, fluoro-pak columns (BioSearch Technologies, FP7210) were coupled with a peristaltic pump; however, the method can be performed by hand according to the fluoro-pak user guide. First, the columns were preconditioned as follows: 8 ml of 100% acetonitrile (MeCN) was passed through the column, followed by 2 ml of TEAA (100 mM) and finally 2 ml of loading buffer (1.71 M NaCl in 5% aqueous *N*,*N*-dimethylformamide). For the conditioning steps, the pump was set to a flow rate of 1 ml/min. Prehybridized sample (see above) was then mixed 1:1 with loading buffer and passed through the column at a rate of 0.4 ml/min. After loading, the resin was subjected to a gradient wash of increasing stringency. The gradient was a mixture of loading buffer and wash buffer (10 mM TEAA in 10% aqueous MeCN), applied in 2 ml increments per column at a rate of 1 ml/min in the following ratios of loading buffer to wash buffer: 85/15, 70/30, 55/45, 30/70 and 15/85. The final wash was typically performed in triplicate for higher scale captures.

Once purified, 2 ml of 100% wash buffer was added to the capped column and placed on a heat block at 85°C for 3 min, and then immediately eluted. The columns proved to be reusable, so they were flushed with 8 ml of 100% MeCN after each use. Samples were butanol concentrated from 2 ml to a volume suitable for ethanol precipitation in a 1.7 ml microcentrifuge tube. The recovered tRNA pellets were resuspended in water and stored at –80°C.

Urea–PAGE analysis

Denaturing–urea PAGE gels (12%, 1.0 mm) were prepared in TBE buffer (1×) and pre-run at 200 V for at least 15 min. A 30 ng aliquot of sample, usually ∼1 μl, was mixed with 10 μl of urea (8 M) dye mixture (xylene cyanol and bromophenol blue, 2×) and diluted to 20 μl with water. The sample was heated at 90°C for 1 min before carefully loading onto the gel, which was run at 200 V for ∼45 min until the xylene cyanol had migrated to the very bottom of the gel. The gel was then carefully removed and stained for 30 min with Sybr Green II (Molecular Probes) as specified by their user guide. Gels were imaged on a BioRad Gel Doc XR, and densitometric analysis was performed using the Image Lab software.

Northern blotting

Approximately 7 × 5 cm^2 sized Hybond N+ nylon membranes (Amersham) were spotted with 3 pmol of captured tRNA that was heat denatured at 90°C for 1 min then blotted onto the membrane, leaving 1 cm between samples. tRNA was then cross-linked to the membrane by irradiating 1200 J of UV radiation using a UV Stratalinker 2400. ULTRAhyb oligo hybridization buffer (Invitrogen) was preheated to 69°C, then 10 ml was added to each dish containing a membrane. The membranes were pre-hybridized for 60 min at 42°C with gentle rocking. The hybridization buffer was removed and 50 μl of biotinylated oligonucleotide probe (1 μM) was added to the buffer, followed by brief mixing. The hybridization buffer was returned to the dish containing a membrane and placed in a shaking incubator at 42°C overnight (∼17 h). The following morning, the membrane was washed with 2 × 10 ml of pre-heated (42°C) NorthernMax High Stringency Wash Buffer (Invitrogen), each wash rocking at 42°C for 15 min. Staining buffer was prepared in the dark by mixing 100 μl of 10% sodium dodecylsulfate (SDS), 50 μl of 20% Tween-20 and 10 μl of IRDye 800 CW Streptavidin (Licor, 926-32230) and diluting to 10 ml in 1× phosphate-buffered saline (PBS) buffer. A 10 ml aliquot of staining buffer was added per membrane followed by tumbling at room temperature in a dark room for 30 min. The staining buffer was discarded and the membranes were washed with 2 × 5 ml of 1× PBS with 1% Tween-20 and tumbled at room temperature in the dark. A third and final wash was performed by adding 5 ml of 1× PBS and tumbling at room temperature for 5 min in the dark. Membranes were then imaged using a Licor Odyssey Fc using the 800 channel and a 2 min integration time.

Calculating tRNA concentration

Total sample absorbance was measured on a NanoDrop spectrophotometer in nucleic acids mode. The raw A_{260} value was input into a web tool (http://biotools.nubic.northwestern.edu/OligoCalc.html) along with the sample sequence to determine the total concentration of the sample. After PAGE analysis, densitometric analysis was performed in order to determine the ratio of the target band intensity within the lane, and this corrected value was multiplied by the total concentration to give the true concentration of the target isoacceptor.

tRNA pre-charging

Homogeneous tRNA samples were enzymatically aminoacylated with AA or ncAA according to a previously reported method (47). When pre-charging natural or isotopic AAs, the charging assay was carried out for 30 min with a final AA concentration of 1 mM. ncAAs on the other hand were charged for 120 min with a final ncAA concentration of 5 mM.

Codon competition assay and sense codon reassignment

All experiments were performed with a customized version of the PURE cell-free translation system (16,48). All translations, unless otherwise specified, were performed on a 30 μl scale for 30 min at 37°C. All AAs and aaRSs required to decode the mRNA were added to the translation with the exception of the leucine–leucyl-tRNA synthetase pair. The final concentration of enzymes in the translation assay were as follows: EF-Tu (10 μM), EF-Ts (8 μM), IF-1 (2.7 μM), IF-2 (0.4 μM), IF-3 (1.5 μM), EF-G (0.52 μM), RF-1 (0.3 μM), RRF (0.5 μM), RF-3 (0.17 μM), ribosomes (1.2 μM), inorganic pyrophosphatase (0.1 μM), creatine kinase (4 μg/ml), nucleoside PP kinase (0.5 mg/ml), myokinase (4

μg/ml) and the aaRSs (0.1–1.0 μM). In order to decode leucine codons, captured or T7 transcribed leucyl-tRNA isoacceptors were pre-charged with leucine or a leucine isotope (d_3, d_7, d_{10} or d_{17}), followed by phenol–chloroform extraction and ethanol precipitation. Pre-charged leucyl-tRNA was then supplemented into the translation mixture at a final concentration of 5 μM, unless otherwise specified. For sense codon reassignment experiments, select leucine tRNA isoacceptors were pre-charged with ncAA (5 mM, pH 7.2) for 2 h at 37°C, purified through phenol–chloroform extraction and ethanol precipitation, and supplemented into translation mixtures at a final concentration of 5 μM. Our mRNA encoded a C-terminal FLAG-tag for anti-FLAG purification, which was performed by adding the translation mixture to 10 μl of anti-FLAG M2 affinity resin (Sigma-Aldrich) and binding on a tumbler for 1 h, before subsequently performing three 500 μl washes with Tris-buffered saline (TBS) buffer and eluting into 1% aqueous trifluoroacetic acid (TFA). The resulting peptides were de-salted via zip-tipping, eluted with a α-cyano-4-hydroxycinnamic acid (CHCA) matrix (1:1 MeCN, 0.2% TFA) and analyzed via MALDI-MS. Quantitative data analysis was performed using ASCII data files.

Quantitation of translation efficiency

Translated peptides were de-salted via C_{18} zip-tip purification and eluted into 7.5 μl of CHCA (10 mg/ml, MeCN/0.1% TFA) before spotting 1 μl on a plate. For each sample, 1000 shots were accumulated and saved as ASCII data files. Mass spectra were then reconstructed using Microsoft excel from the ASCII files. For quantitation, the peak height maxima associated with the expected peptide [M + H]+ were acquired from the ASCII data files and directly compared (49,50).

RESULTS

A new method for the capture of tRNA isoacceptors from total tRNA

Purification of a single tRNA from a cellular pool of RNA requires removal of numerous structurally similar contaminant tRNAs (46 total tRNAs in *E. coli*). Furthermore, the conservation of higher order structure across all tRNAs within an organism makes tRNA capture via hybridization a challenge (51,52). Despite these challenges, we sought to develop a tRNA capture method that was highly stringent and scalable, while still offering enough versatility to be applicable towards isolation of any tRNA. To this end, we developed a two-step process. First, *E. coli* total tRNA was denatured in the presence of a fluorous-modified antisense oligonucleotide, forming a target–oligo duplex (Figure 1A). Next, the mixture was loaded onto a fluorous affinity column, where the target–oligo duplex is retained through fluorous–fluorous interactions while non-duplexed RNA is washed off the column, followed by simple heat denaturation of the duplex to release the target into the eluant while retaining the oligo on the column (Figure 1B).

Our first fluorous-tagged oligos were derived from the northern blotting probes reported by Dong and Kurland (46), labeled with a fluorous ponytail at the 3′ end. We initially observed better capture results with target–oligo duplexes having higher T_ms, motivating us to redesign a new set of longer oligos spanning the variable loop and anticodon–stem loop, which we accordingly named the variable loop oligos (V loop) (Figure 1A). However, most tRNAs carry PTMs in the anticodon stem–loop that are probable hydrogen bond disruptors, such as 1-methylguanosine (single letter abbreviation K, Figure 1B). This prompted us to design a second set of oligos, focusing instead on the 5′ acceptor stem through the D stem–loop, which primarily carries PTMs that do not influence intermolecular hydrogen bonding, such as dihydrouridine (single letter abbreviation D, Figure 1B). Accordingly, we named these the D loop oligos; sequences of each oligo design and corresponding T_ms can be found in Supplementary Table S1. While both oligo designs resulted in successful tRNA isolation, we preferred the performance of the D loop oligos, which resulted in better purification yields. Indeed, computational screening of the global energy minimum between select tRNAs and their corresponding oligos confirmed that the D loop oligos form more stable duplexes than the Dong and Kurland oligos (RNAstructure bifold, Supplementary Figure S1) (53).

To evaluate the versatility of the tRNA capture method, it was tested without customization against 27 out of 46 *E. coli* tRNA isoacceptors from the leucine, serine, arginine, glycine, proline, valine, threonine, alanine, isoleucine and phenylalanine families. PAGE analysis revealed an 85% success rate, with 23 out of 27 captured tRNAs showing highly purified bands with anticipated migration patterns (Figure 2A, B; Supplementary Figure S2). While small contaminant bands were revealed by PAGE in certain cases, the migration of these bands was not in the tRNA region, with the exception of several tRNA leucine isoacceptors and tRNA Val 2. In the case of the leucyl isoacceptors, such bands were eliminated upon switching to D loop oligos (Figure 2B), which suggested that the lower bands were tRNA fragments lacking nucleotides at the 5′ end. tRNA Val 2a has a highly similar isoacceptor, tRNA Val 2b, which is probably captured with Val 2a due to sequence homology and could explain the observed contaminant band seen with tRNA Val 2a (Figure 2A). These results suggest that in most cases, our tRNA capture method is ‘plug and play’; however, in cases where tRNAs prove elusive or insufficiently pure, protocol optimization and oligonucleotide design can lead to improved performance.

To further examine the purity of captured tRNAs, the five leucyl-tRNA isoacceptors were subjected to enzymatic screening. Each isoacceptor tRNA was captured and separately carried through an aminoacylation charging assay in the presence of all 20 canonical amino acids and aaRSs (47). This assay measures the presence of the aminoacyl-tRNA bond through derivatization and digestion with cleavage with nuclease P1. If tRNAs corresponding to other AAs are present, these plots would show a multitude of peaks since the aaRS enzymes would charge these contaminant tRNAs with their cognate (but non-leucine) AAs (47). MALDI-MS analysis revealed a major peak corresponding to the expected mass of derivatized Leu-AMP for each of the five isoacceptors, confirming the leucyl identity of each tRNA (Figure 2C). Furthermore, MALDI analysis did not show

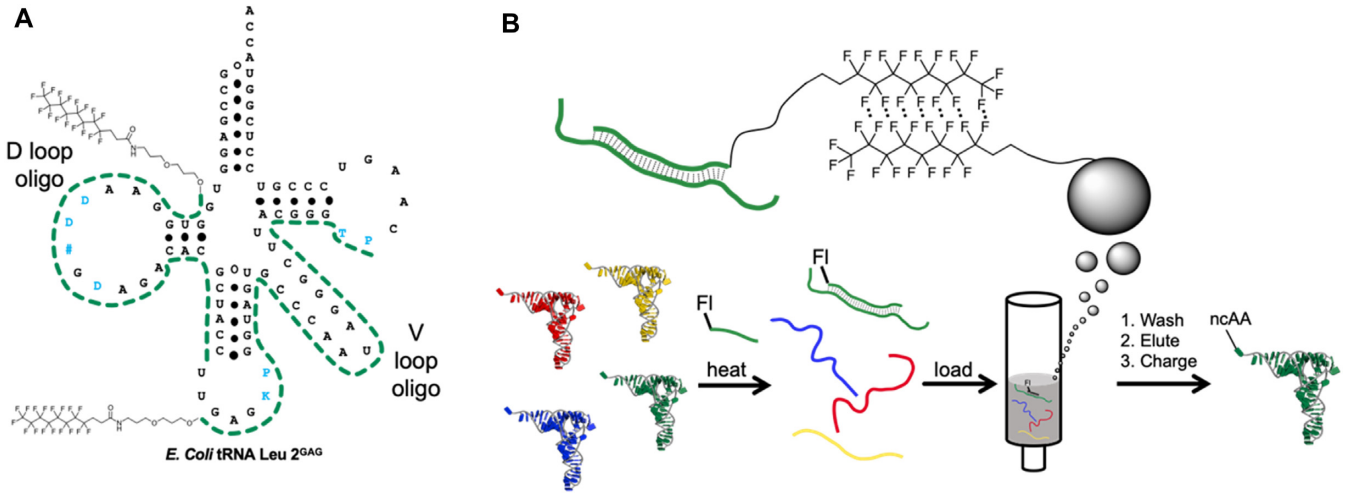

Figure 1. Development of a fluorous capture method for tRNA isolation. (**A**) The secondary structure of tRNA Leu 2^{GAG} with two different oligonucleotide target regions, each of which is shown with a fluorous tag. Post-transcriptionally modified nucleotides are depicted in blue with their single letter abbreviations (D = dihydrouridine, # = 2′-*O*-methylguanidine, K = 1-methylguanidine, P = pseudouridine, T = 5-methyluridine). (**B**) tRNA capture method, beginning with liquid-phase hybridization of heterologous cellular RNA with a fluorous-tagged oligo complementary towards a single target and followed by fluorous affinity chromatography. After purification, the tRNA was charged with a canonical AA or ncAA using the appropriate aaRS.

peaks that match the expected mass of any of the other 19 aminoacylation profiles (Figure 2C). Finally we analyzed each of the purified Leu isoacceptors using northern blotting with isoacceptor-selective probes (Figure 2D). Each of the tRNAs was highly pure and not contaminated with significant amounts of the other isoacceptors (Figure 2D; Supplementary Figure S3). These results combined with PAGE analysis demonstrate the selectivity of our tRNA capture method, which delivers a broad range of highly purified tRNA isoacceptors.

Having established the method's versatility and selectivity, we aimed to improve its throughput and ease of use. We built a custom rack from parts available at any home goods store and paired it with a peristaltic pump, allowing the partially automated use of up to eight columns at once (Supplementary Figure S4). Each column has a loading capacity up to 0.2 μmol, prompting us to test the scalability of the capture method. By simply scaling up each component of the hybridization mixture, and employing a gradient rather than an isocratic wash method, we frequently captured each leucyl-tRNA isoacceptor in the low to mid nanomolar range (Supplementary Figure S5). We believe our method could be scaled even further; however, due to reagent costs, we never approached the theoretical fluorous loading capacity of the columns. At the highest scale tested (15 nmol oligonucleotide added), we did not observe any bleeding of fluorous oligonucleotide in the column flowthrough using UV-Vis absorbance (not shown, LOD 0.5%). The capture method can, therefore, be made more cost-effective by collecting rather than discarding the flowthrough, adding a new oligo and repeating the protocol (Supplementary Figure S6). We have also reused the same fluorous columns dozens of times without losses in efficiency. A problem occasionally observed at the highest scales is that a small amount of the fluorous oligonucleotide will co-elute with the tRNA. In these cases, the simple remedy is to pass the mixture back through a fresh column.

Evaluation of the translation efficiency of wt versus t7tRNA

With access to purified wt tRNAs, we set out to better understand their translational capabilities compared with t7tRNA counterparts. With few exceptions, experiments that evaluate the codon reading specificities of tRNAs have focused on testing the tRNA in the absence of any competitors. We desired a method where we could simply compare the efficiencies of a wt versus t7tRNA for a given codon in a competitive format (Figure 3A). We reasoned that these types of experiments could be carried out by charging isotopically labeled versions of amino acids onto each tRNA, and supplementing them equally into a PURE translation with an mRNA containing one variable leucine codon. The resulting peptides would then have a mass difference equal to the difference between the mass of the leucine isotopes, allowing direct comparison of decoding efficiencies by MALDI-MS analysis.

Our process relied upon independent charging of each tRNA at equal concentrations, which were mixed prior to phenol– chloroform extraction in order to maintain an equal tRNA ratio. The tRNA concentration was determined as described in the Materials and Methods and Supplementary Figure S7. To confirm this approach, we analyzed via MALDI-MS the aminoacylation profiles of a tRNA mixture containing Leu-t7tRNA Leu 5 and d_{10}-Leu-wt tRNA Leu 5. The mass spectra showed nearly identical peak intensities for the two peaks corresponding to each acylated tRNA, confirming that our approach would not bias competition results due to unequal tRNA concentrations (Figure 3B).

The codon competition assay was then performed for every known (46) pairing between leucine codons and their cognate tRNAs. We charged wt tRNAs with d_{10} leucine whereas t7tRNAs received non-isotopic leucine. The resulting mass spectra showed much greater peak intensity for peptides bearing d_{10} leucine, indicating greater codon

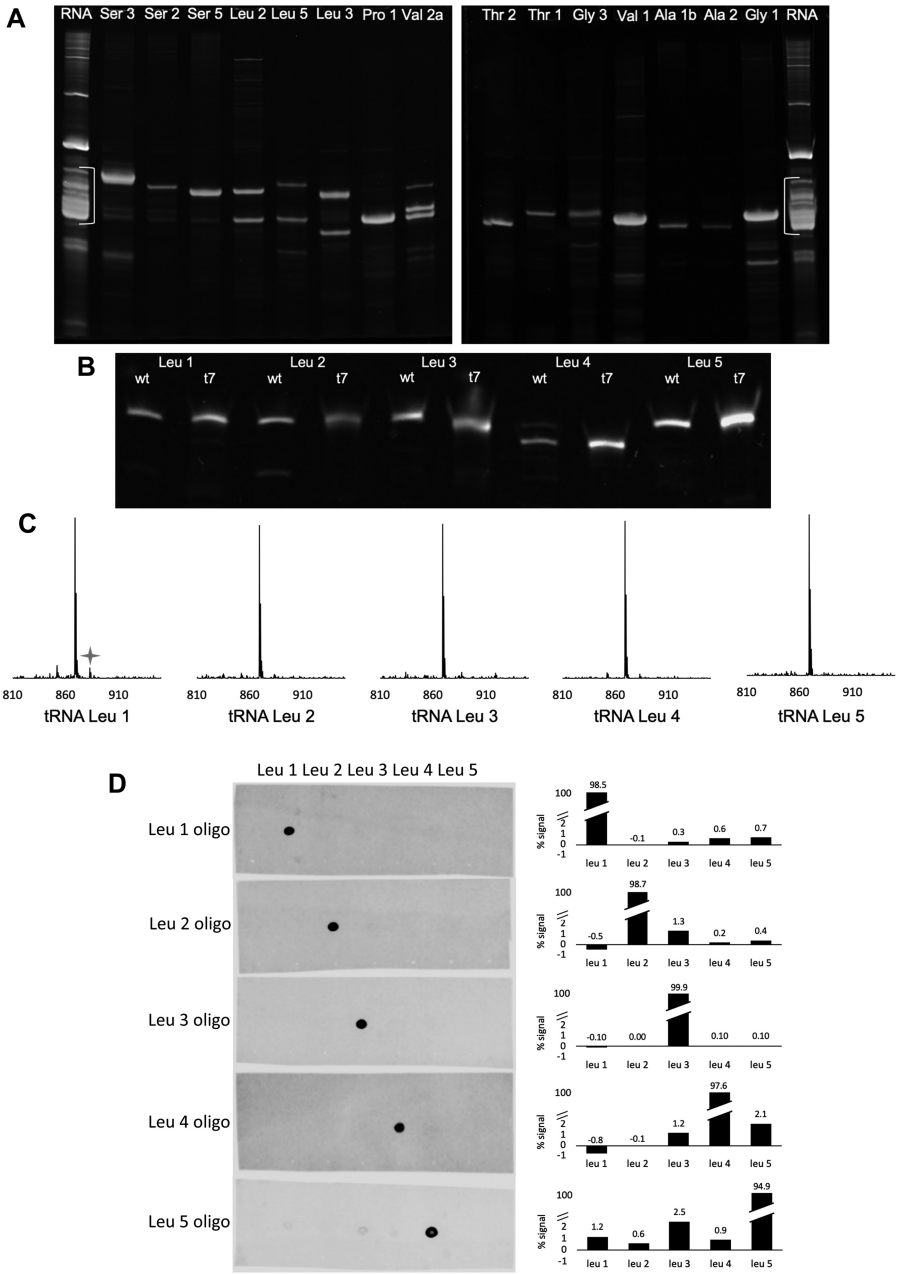

Figure 2. Fluorous capture leads to homogeneous populations of the desired tRNAs in most cases. (**A**) Urea–PAGE analysis of 15 miscellaneous tRNA isoacceptors isolated using the described method, flanked by the starting cellular RNA on each end of the gels. The total tRNA region of the cellular RNA is shown with white brackets. (**B**) Urea–PAGE analysis of all five leucyl-tRNAs (wt) captured with D loop oligos, next to their t7tRNA counterparts (t7). (**C**) MALDI-MS analysis of aminoacylation profiles of each of the five purified leucine isoacceptors charged with all 20 canonical amino acids and aaRSs. The gray star denotes the very small +14 peak that is an occasional byproduct of the assay resulting from reaction of the AA-tRNA with trace amounts of formaldehyde present in the methanolic solution used for the derivatization reaction (47). This peak does not correspond to the mass of any of the canonical AA-AMPs. (**D**) Dot blot northern analysis of tRNA isoacceptor purity. A 30 pmol sample of each tRNA isoacceptor was spotted on a positively charged nylon membrane and blotted with one of five isoacceptor-specific biotinylated probes labeled and imaged with IR800-labeled streptavidin. The plot on the right has broken axes in order to visualize the small amounts of contaminating tRNAs present (see also Supplementary Figure S3). tRNA numbering is from Dong and Kurland (46).

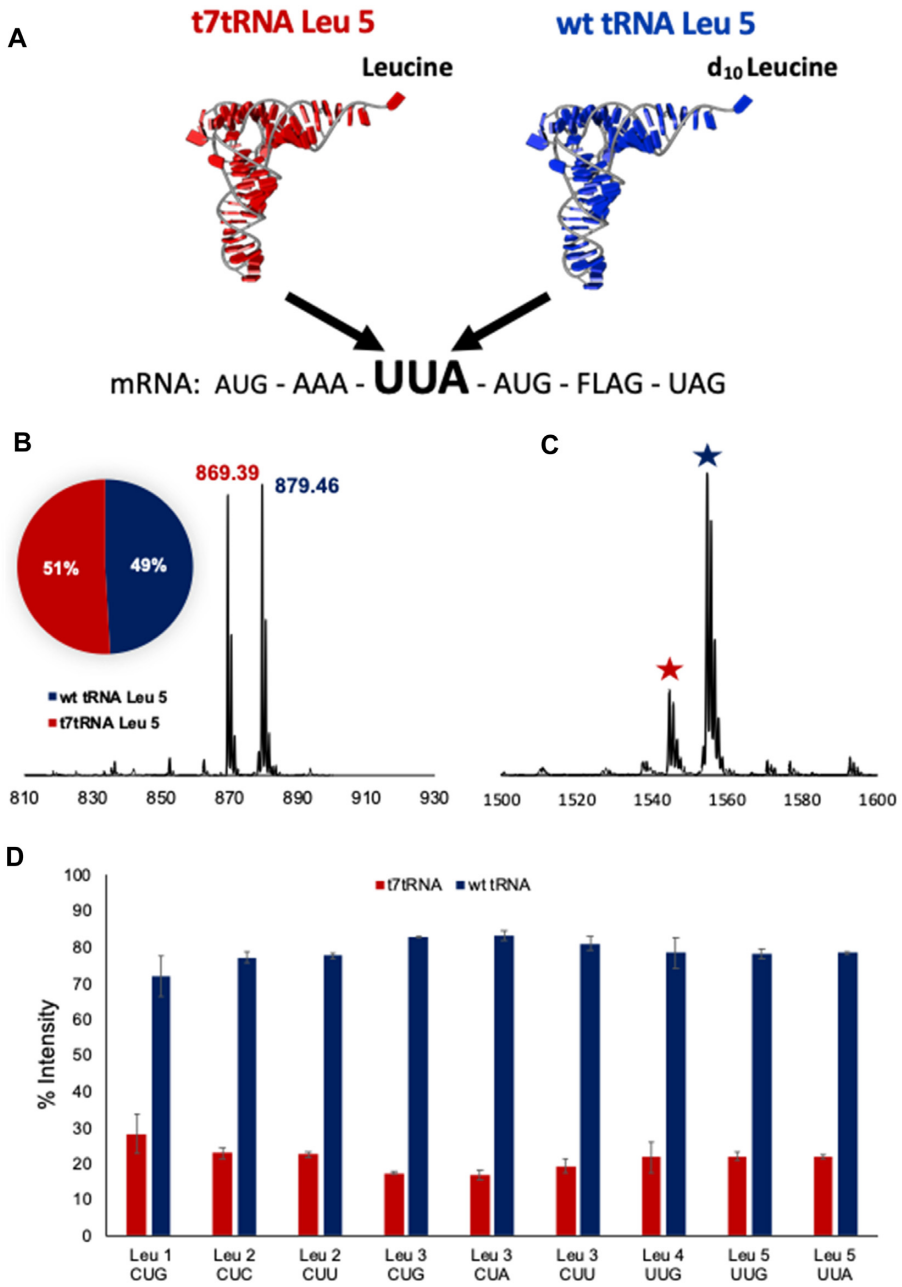

Figure 3. Direct competition assay between wt and t7tRNA for a cognate codon. (**A**) Representation of the competition between isotopically charged wt and t7tRNA Leu 5, for their cognate UUA codon in an mRNA. mRNAs were designed for each of the six leucine codons, replacing the UUA codon with a codon of interest. (**B**) Mass spectra of a mixture of wt and t7tRNA Leu 5 prepared for codon competition experiments, with aminoacylation profiles revealing the desired balance between tRNAs required for unbiased codon competition experiments. (**C**) Mass spectra showing the translation results of a codon competition experiment between wt and t7tRNA Leu 5 for the UUA codon. (**D**) Quantitative comparison of the peptide peak intensities corresponding to either t7tRNA readthrough (red) or wt tRNA readthrough (blue). Error bars denote the standard deviations of at least three independent experiments.

readthrough by wt tRNA (Figure 3C; Supplementary Figure S8). Quantitative comparison of the peptide peaks corresponding to wt and t7tRNA readthrough revealed a unanimous 3- to 4-fold preference for wt tRNA over t7tRNA (Figure 3D). While most SCR applications utilize t7tRNA for mRNA decoding, our results suggest that various components of the translation system prefer wt tRNA due to their PTMs. We suspected that such discrepancies in tRNA preference would only be accentuated with the involvement of ncAA.

Sense codon reassignment using either wt or t7tRNA

In order to successfully reassign sense codons, orthogonal groupings of tRNA isoacceptors that do not compete for the same codon must be selected. Based on previously estab-

lished leucine codon readthrough patterns, we designed two SCR schemes using two different mRNAs, each encoding three different leucine codons. Scheme 1 featured adjacently placed CUC, CUA and UUA codons in mRNA 1 (Figure 4A). To orthogonally decode these codons, we used a tRNA mixture comprised of Leu 2/3/5 pre-charged with ß-*tert*-butyl-L-alanine (tBuAla), trifluoroleucine (F_3Leu) and leucine (Leu), respectively (Figure 4A, B). Non-leucine codons were decoded by *in situ* charged total tRNA with the corresponding AA–AARS pairs within the PURE translation system. The ability to achieve SCR as described in scheme 1 was tested using a mixture of either wt or t7 tRNA Leu 2/3/5, or entirely with *in situ* charging with no ncAA as a control. For the wt tRNA mixture, MALDI-MS analysis revealed a major peak corresponding to the expected mass of the desired peptide (Figure 4C). Minor peaks were observed corresponding to mistranslation events, suggesting incomplete codon orthogonality (Figure 4C). The t7tRNA mixture, on the other hand, showed nearly equal translation of the desired peptide and a mistranslated peptide where the CUA codon is misread by tRNA Leu 2, adding an additional F_3Leu to the peptide (Figure 4C). While the translation yields of the wt and t7tRNA mixtures were nearly equal (Supplementary Figure S9), the mass spectra highlight the difficulties of ncAA incorporation through SCR using t7tRNA.

To better understand the flexibility of SCR, a second SCR scheme was designed using a new set of leucine codons. Scheme 2 featured adjacent CUU, CUG and UUG codons in mRNA 2, which were orthogonally decoded using a tRNA mixture comprised tRNA Leu 1/2/5 pre-charged with tBuAla, F_3Leu and Leu. respectively (Figure 5A, B). mRNA 2 was subjected to the same experimental design as mRNA 1. As previously observed with mRNA 1, MALDI-MS analysis of the translation results using the wt tRNA mixture showed a major peak corresponding to the expected mass of the desired peptide (Figure 5C), with other peaks being very minor (Figure 5C). Decoding mRNA 2 with the t7tRNA mixture, on the other hand, showed more significant mistranslation compared with the mRNA 1 experiments, producing a major peak corresponding to a mistranslated peptide where the UUG codon is misread by Met-tRNA^{Met} rather than Leu-tRNA$^{Leu\ 5}$ (Figure 5C).

While we were surprised by the Met mistranslation, the inability of t7tRNA Leu 5 to read the UUA codon has been noted before (21). Indeed, by making a new t7tRNA mixture with wt tRNA Leu 5 in place of t7tRNA Leu 5, the desired peptide was restored and the mistranslated methionine peptide diminished; however, a new peak was observed corresponding to wt tRNA Leu 5 outcompeting t7tRNA Leu 1 for the CUG codon (Supplementary Figure S10). These results demonstrate the delicate balance needed to break codon degeneracy and underscore the usefulness of wt tRNA for SCR.

DISCUSSION

An important achievement of our work is the development of a new fluorous capture method for the isolation of homogeneous tRNA isoacceptors (Figure 1). While our tRNA capture method provided most of the utility we desired, tRNAs Ile 2 and Arg 3/4/5 evaded capture attempts. To better understand this, we first checked to see if any hydrogen bond disrupting PTMs existed within the hybridization region of these tRNAs; however, such modifications are found exclusively within the anticodon loop, which the D loop oligos do not target (Figure 1A; Supplementary Figure S11) (54). We then questioned whether the target–oligo duplex was stable enough to remain folded throughout the capture protocol. To examine this quantitatively, we used the RNAstructure bifold web server to calculate the folding energy between tRNA targets and their complementary oligo, permitting intramolecular base pairing to simulate global minimum confirmations (53). Calculations revealed that tRNAs we failed to capture folded with their complementary oligo with an average calculated ΔG value + 19.76 kcal/mol higher than the leucine tRNA isoacceptors, which were regularly captured (Supplementary Figure S12). We hypothesize that ΔG oligo optimization would permit the capture of an even broader scope of tRNAs. Other strategies for enhancing the stability of the target–oligo duplex include designing oligos comprised of custom nucleotides, such as 2′*O*-Me, locked nucleic acids or peptide nucleic acids.

Our applications dictated the use of our capture method exclusively to isolate tRNA; however, it should be straightforward to apply this strategy to the purification of other nucleic acids spanning a range of organisms. One such class of targets are non-coding RNAs (ncRNAs), which are emerging as novel biomarkers (55). With thousands of ncRNAs transcribed from the human genome, versatile isolation methods are needed, making our capture method appealing compared with solid-phase hybridization approaches (55,56). While such clinically derived samples will have a more complex matrix than our total tRNA source, simple purification steps should rescue performance should the matrix prove challenging. Furthermore, even small ncRNA should form stable enough duplexes with fluorous oligos to survive our washing procedure. Improved access to ncRNA should accelerate new discoveries in human health as well as the development of better diagnostics.

In contrast to t7tRNA, cellular tRNA is decorated with numerous PTMs. The *E. coli* leucyl-tRNA isoacceptors alone carry 10 unique modifications across the tRNA core and anticodon stem–loop regions (Figure 6). PTMs to the leucyl-tRNA core include dihydrouridine (D), 4-thiouridine (4), pseudouridine (P), 2′-*O*-methylguanosine (#) and 5-methyluridine (T, ribothymidine). tRNA core PTMs are much more commonly conserved than anticodon PTMs and are known to play important roles in tRNA stability and integrity of the tertiary, L-shaped structure (57). Five unique PTMs are decorated across the anticodon loops of some but not all leucyl-tRNAs, including uridine-5-oxyacetic acid (V), 2′-*O*-methylcytidine (B) and 5-carboxymethylaminomethyl-2′-*O*-methyluridine,) at the 34th nucleotide position, and 1-methylguanosine (K) or 2 methylthio-N^6-isopentenyladenosine (*) at the 37th nucleotide position (Figure 6). The V modification in tRNA Leu 3 likely contributes to its ability to read the CUU codon, which involves a non-Watson–Crick U–U base pair, and in general PTMs at the 34th wobble position regulate codon recognition (58). PTMs at the 37th position help confer structural order to the anticodon and assist in A-site binding and prevention of frameshifting (34,57,59).

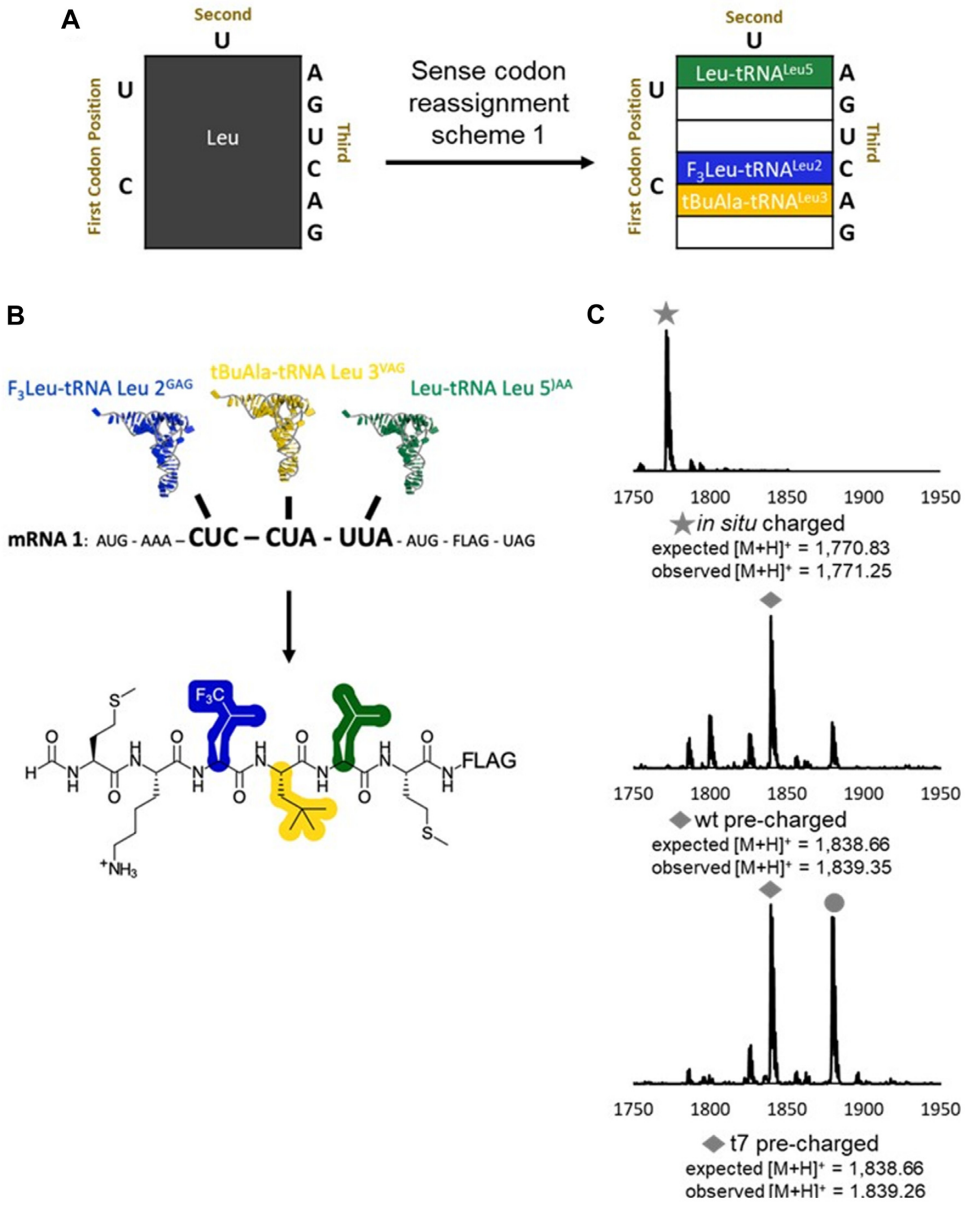

Figure 4. Translation of a peptide featuring two ncAAs through reassignment of the CUC, CUA and UUA leucine codons. (**A**) Reassignment of the 6-fold degenerate leucine codon box to encode Leu, F_3Leu and tBuAla. The gray box on the left reflects the degenerate encoding of a single amino acid, whereas the green, blue and yellow colors on the right correspond to the identity of the tRNA bearing each amino acid. White codon boxes are unused in the scheme. (**B**) Decoding of the three leucine codons in mRNA 1 by their cognate tRNAs, each aminoacylated with a unique amino acid monomer resulting in the translation of the target peptide (ncAA side chains are highlighted). Modified nucleotides within the anticodon are represented by their single letter codes V = 5-oxyacetic acid uridine,) = 5-carboxymethylaminomethyl-2′-*O*-methyluridine). (**C**) MALDI-MS spectra of the sense codon reassignment experiments, using *in situ* charged leucyl-tRNA (top), pre-charged leucyl wt tRNA (middle) or pre-charged leucyl t7tRNA (bottom). Expected masses of the peptide products are depicted with either a star or a diamond, as denoted under each spectrum. The large peak in the t7 reassignment scheme (denoted with a circle) corresponds to tRNA Leu 2 reading the CUA codon.

Direct competition of wt leucyl-tRNA isoacceptors against their t7tRNA counterparts for cognate codons revealed a 3- to 4-fold higher readthrough by wt tRNAs (Figure 3D). This could be caused by differences in binding to EF-Tu-GTP. The binding affinity of EF-Tu for AA-tRNA is the sum of the interactions between EF-Tu and the amino acid, as well as interactions with the tRNA, predominantly certain nucleotides in the T-stem (32). Although the EF-Tu affinity of modified versus unmodified tRNA Leu has not been studied to our knowledge, studies with other tRNAs have shown up to 3-fold losses in affinity for EF-Tu-GTP when modifications are removed (31,60). If a ncAA weakens the interaction with EF-Tu, introducing that ncAA onto a t7tRNA will be likely to compound this effect, resulting in weakened ternary complex formation and hindered translocation to the ribosome. Current literature around mutating the T-stem and the frequent need for the addition of high ncAA-tRNA concentrations in translation both support

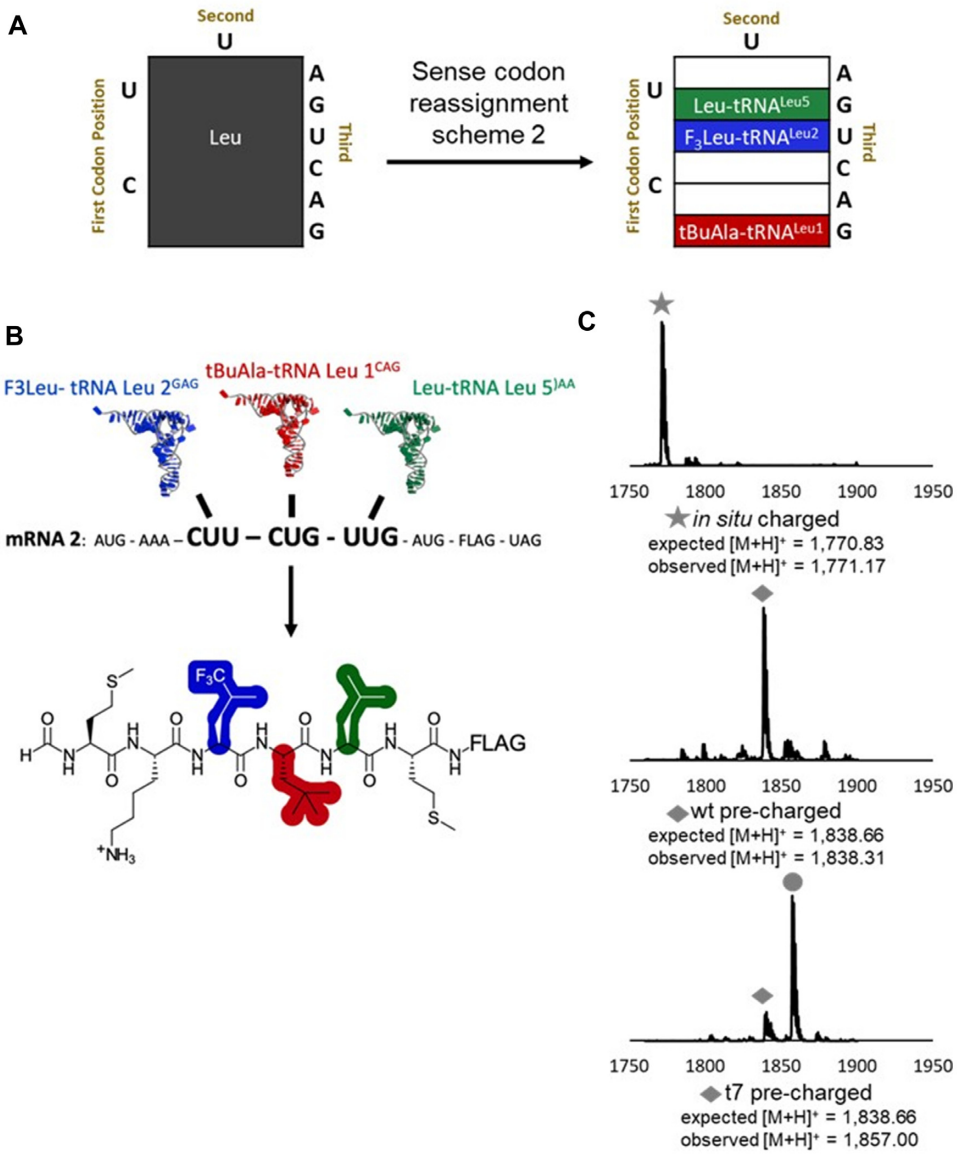

Figure 5. Translation of a peptide featuring two ncAAS through reassignment of the CUU, CUG and UUG leucine codons. (**A**) Reassignment of the 6-fold degenerate leucine codon box to encode Leu, F_3Leu and tBuAla. The gray box on the left reflects the degenerate encoding of a single amino acid, whereas the green, blue and red colors on the right correspond to the identity of the tRNA bearing each amino acid. White codon boxes are unused in the scheme. (**B**) Decoding of the three leucine codons in mRNA 2 by their cognate tRNAs, each aminoacylated with a unique amino acid monomer resulting in the translation of the target peptide (ncAA side chains are highlighted). Modified nucleotides within the anticodon are represented by their single letter codes () = 5-carboxymethylaminomethyl-2′-*O*-methyluridine). (**C**) MALDI-MS spectra of the sense codon reassignment experiments, using *in situ* charged leucyl-tRNA (top), pre-charged leucyl wt tRNA (middle), or pre-charged leucyl t7tRNA (bottom). Expected masses of the peptide products are depicted with either a star or a diamond. The largest peak in the t7 reassignment corresponds to a misincorporation of methionine (denoted with a circle).

these notions (42,61,62). Another possible explanation for the higher readthrough by wt tRNA is differences in accommodation between wt and t7tRNA/EF-Tu/GTP ternary complexes at the A-site of the ribosome. It was shown that t7tRNAs lacking PTMs at the 34th and 37th nucleotide positions enter the ribosomal binding site with greater conformational freedom within the anticodon stem–loop, creating an entropic penalty the ribosome must pay in order to bind and sample the ternary complex-bound tRNA (35). Elimination of the *N*-1 methyl group on guanosine (Figure 6, nucleotide K) also causes ribosomal stalling at CUA and other codons (59). Our work highlights the effects these post-transcriptional modifications have on translation with ncAAs and supports the advantages of fully modified tRNAs for sense codon reassignment. Access to homogeneous isoacceptor populations will enable further studies of the effects of these modifications on all aspects of translation.

Reported strategies for sense codon reassignment have utilized a wide range of codon families. The majority of these studies focus on adding just one ncAA per codon box. In order for sense codon reassignment to realize its full potential, strategies for encoding multiple ncAAs from within

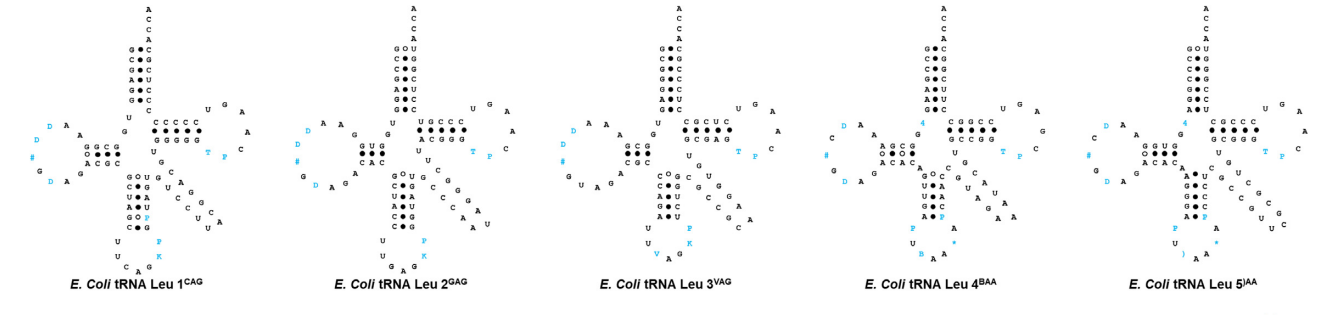

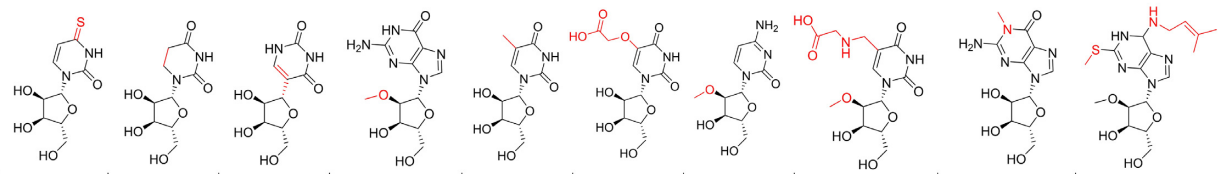

	4	D	P	#	T	V	B	)	K	*
Leu 1		**16**, 17, 20	38, 40, **55**	**18**	**54**				37	
Leu 2		**16**, 17, 20	38, **55**	**18**	**54**				37	
Leu 3		**16**, 17	38, **55**	**18**	**54**	34			37	
Leu 4	8	**16**, 20	32, 39, **55**	**18**	**54**		34			37
Leu 5	8	**16**, 20	32, 39, **55**	**18**	**54**			34		37

tRNA body modification position #s

tRNA anticodon stem-loop modification position #s

Figure 6. List of the modified bases for the *E. coli* leucyl-tRNA isoacceptors. Cloverleaf structures of all five leucyl-tRNAs (top), with modification single letter codes shown as blue text, Watson–Crick base pairs shown as filled dots and non-Watson–Crick pairing shown as open dots. Chemical structures of each modification are shown below, along with the nucleotide position of each modification (bottom) on each tRNA isoacceptor. Modifications that are site specifically conserved in *E. coli* leucyl-tRNA are shown in bold, black text. Modification identity, name, structure and location were found on the Modomics webserver [4 = 4-thiouridine, D = dihydrouridine, P = pseudouridine, # = 2′-*O*-methylguanosine, T = 5-methyuridine, V = uridine-5-oxyacetic acid, B = 2′-*O*-methylcytidine,) = 5-carboxymethylaminomethyl-2′-*O*-methyluridine, K = 1- methylguanosine, * = 2-methylthio-N^6-isopentenyladenosine] (63).

the same codon box are needed. We have described, to the best of our knowledge, the first examples where the 6-fold degenerate leucine codon family (Figures 4C and 5C) was engineered to encode three AAs. Moreover, we have developed a generalizable strategy for isolating wt tRNAs and competitive readthrough testing of tRNAs that will enable rapid testing of future tRNAs for their capabilities for GCE.

SUMMARY

In summary, we describe the development of a novel tRNA capture method combining liquid-phase antisense hybridization and fluorous affinity chromatography. Without any protocol alterations, we demonstrated the successful application of this method towards 23 out of 27 targeted tRNAs. Furthermore, we show that our method can be made partially automated, high-throughput, easily scalable and can be implemented with cost-saving recycled reagents. We show that wt tRNAs outcompete their t7tRNA counterparts for cognate codons, winning the codon around 3–4 times more often than the t7tRNA. Finally, we show that the 6-fold degenerate leucine codon family can be reassigned to encode three amino acid monomers, including two ncAAs, using two schemes that each pair three different leucine codons together. Wt tRNA, but not t7tRNA, was discriminated with enough fidelity to execute these sense codon reassignment schemes and support the biosynthesis of a peptide bearing two ncAAs in a PURE translation system.

DATA AVAILABILITY

The data underlying this article will be shared on reasonable request to the corresponding author.

SUPPLEMENTARY DATA

Supplementary Data are available at NAR Online.

ACKNOWLEDGEMENTS

The authors are grateful to H.E.O. Franco, B. Shakya, A. Le, C. Makovsky and G. Kerestesy for helpful comments on the manuscript. We thank P. Dent (VCU) and L. Booth (VCU) for use of the Li-Cor Odyssey imager.

FUNDING

National Institute of General Medical Sciences (NIGMS) [R01GM143396] and National Cancer Institute [R03CA216116]. Funding for open access charge: NIGMS.
Conflict of interest statement. M.C.T.H and C.M have applied for a provisional patent on the fluorous capture strategy.

REFERENCES

1. Noren,C.J., Anthony-Cahill,S.J., Griffith,M.C. and Schultz,P.G. (1989) A general method for site-specific incorporation of unnatural amino acids into proteins. *Science*, **244**, 182–188.
2. de la Torre,D. and Chin,J.W. (2021) Reprogramming the genetic code. *Nat. Rev. Genet.*, **22**, 169–184.
3. Davis,L. and Chin,J.W. (2012) Designer proteins: applications of genetic code expansion in cell biology. *Nat. Rev. Mol. Cell Biol*, **13**, 168–182.
4. Hacker,D.E., Hoinka,J., Iqbal,E.S., Przytycka,T.M. and Hartman,M.C.T. (2017) Highly constrained bicyclic scaffolds for the discovery of protease-stable peptides via mRNA display. *ACS Chem. Biol.*, **12**, 795–804.
5. Walport,L.J., Obexer,R. and Suga,H. (2017) Strategies for transitioning macrocyclic peptides to cell-permeable drug leads. *Curr. Opin. Biotechnol.*, **48**, 242–250.
6. Poongavanam,V., Doak,B.C. and Kihlberg,J. (2018) Opportunities and guidelines for discovery of orally absorbed drugs in beyond rule of 5 space. *Curr. Opin. Chem. Biol.*, **44**, 23–29.
7. Viarengo-Baker,L.A., Brown,L.E., Rzepiela,A.A and Whitty,A. (2021) Defining and navigating macrocycle chemical space. *Chem. Sci.*, **12**, 4309–4328.
8. Muttenthaler,M., King,G.F., Adams,D.J and Alewood,P.F. (2021) Trends in peptide drug discovery. *Nat. Rev. Drug. Discov.*, **20**, 309–325.
9. Tharp,J.M., Vargas-Rodriguez,O., Schepartz,A. and Soll,D. (2021) Genetic encoding of three distinct noncanonical amino acids using reprogrammed initiator and nonsense codons. *ACS Chem. Biol.*, **16**, 766–774.
10. Italia,J.S., Addy,P.S., Erickson,S.B., Peeler,J.C., Weerapana,E. and Chatterjee,A. (2019) Mutually orthogonal nonsense-suppression systems and conjugation chemistries for precise protein labeling at up to three distinct sites. *J. Am. Chem. Soc.*, **141**,6204–6212.
11. Dunkelmann,D.L., Oehm,S.B., Beattie,A.T. and Chin,J.W. (2021) A 68-codon genetic code to incorporate four distinct non-canonical amino acids enabled by automated orthogonal mRNA design. *Nat. Chem.*, **13**, 1110–1117.
12. DeBenedictis,E.A., Carver,G.D, Chung,C.Z., Söll,D. and Badran,A.H. (2021) Multiplex suppression of four quadruplet codons via tRNA directed evolution. *Nat. Commun.*, **12**, 5706.
13. Neumann,H., Wang,K., Davis,L., Garcia-Alai,M. and Chin,J.W. (2010) Encoding multiple unnatural amino acids via evolution of a quadruplet-decoding ribosome. *Nature*, **464**, 441–444.
14. Dien,V.T., Morris,S.E., Karadeema,R.J. and Romesberg,F.E. (2018) Expansion of the genetic code via expansion of the genetic alphabet. *Curr. Opin. Chem. Biol.*, **46**, 196–202.
15. Hoshika,S., Leal,N.A., Kim,M.J., Kim,M.S., Karalkar,N.B., Kim,H.J., Bates,A.M., Watkins,N.E., Santalucia,H.A., Meyer,A.J. *et al.* (2019) Hachimoji DNA and RNA: a genetic system with eight building blocks. *Science*, **363**, 884–887.
16. Shimizu,Y., Inoue,A., Tomari,Y., Suzuki,T., Yokogawa,T., Nishikawa,K. and Ueda,T. (2001) Cell-free translation reconstituted with purified components. *Nat. Biotechnol*, **19**, 751–755.
17. Hammerling,M.J., Krüger,A. and Jewett,M.C. (2020) Strategies for in vitro engineering of the translation machinery. *Nucleic Acids Res.*, **48**, 1068–1083.
18. Josephson,K., Hartman,M.C.T. and Szostak,J.W. (2005) Ribosomal synthesis of unnatural peptides. *J. Am. Chem. Soc.*, **127**, 11727–11735.
19. Richardson,S.L, Dods,K.K., Abrigo,N.A, Iqbal,E.S. and Hartman,M.C.T. (2018) In vitro genetic code reprogramming and expansion to study protein function and discover macrocyclic peptide ligands. *Curr. Opin. Chem. Biol.*, **46**, 172–179.
20. Peacock,H. and Suga,H.i (2021) Discovery of de novo macrocyclic peptides by messenger RNA display. *Trends Pharm. Sci.*, **42**, 385–397.
21. Cui,Z., Stein,V., Tnimov,Z., Mureev,S. and Alexandrov,K. (2015) Semisynthetic tRNA complement mediates in vitro protein synthesis. *J. Am. Chem. Soc*, **137**, 4404–4413.
22. Iwane,Y., Hitomi,A., Murakami,H., Katoh,T., Goto,Y. and Suga,H. (2016) Expanding the amino acid repertoire of ribosomal polypeptide synthesis via the artificial division of codon boxes. *Nat. Chem.*, **8**, 317–325.
23. Lin,C.W, Harner,M.J., Douglas,A.E., Lafont,V., Yu,F., Lee,V.G., Poss,M.A., Swain,J.F., Wright,M. and Lipovšek,D. (2021) A selection of macrocyclic peptides that bind STING from an mRNA-Display library with split degenerate codons. *Angew. Chem. Int. Ed.*, **60**, 22822–22827.
24. Kwon,I. and Choi,E.S. (2016) Forced ambiguity of the leucine codons for multiple-site-specific incorporation of a noncanonical amino acid. *PLoS One*, **11**, e0152826.
25. Bohlke,N. and Budisa,N. (2014) Sense codon emancipation for proteome-wide incorporation of noncanonical amino acids: rare isoleucine codon AUA as a target for genetic code expansion. *FEMS Microbiol. Lett.*, **351**, 133–144.
26. Fredens,J., Wang,K., De La Torre,D., Funke,L.F.H., Robertson,W.E., Christova,Y., Chia,T., Schmied,W.H., Dunkelmann,D.L., Beránek,V. *et al.* (2019) Total synthesis of *Escherichia coli* with a recoded genome. *Nature*, **569**, 514–518
27. Robertson,W.E, Funke,L.F.H., de la Torre,D., Fredens,J., Elliott,T.S, Spinck,M., Christova,Y., Cervettini,D., Böge,F. and Liu,K.C. (2021) Sense codon reassignment enables viral resistance and encoded polymer synthesis. *Science*, **372**, 1057–1062.
28. Lee,K.B., Hou,C.Y., Kim,C.E, Kim,D.M, Suga,H. and Kang,T.J. (2016) Genetic code expansion by degeneracy reprogramming of arginyl codons. *ChemBioChem*, **17**, 1198–1201.
29. Blanchet,S., Cornu,D., Hatin,I., Grosjean,H., Bertin,P. and Namy,O. (2018) Deciphering the reading of the genetic code by near-cognate TRNA. *Proc. Natl Acad. Sci. USA*, **115**, 3018–3023.
30. Eargle,J., Black,A.A., Sethi,A., Trabuco,L.G. and Luthey-Schulten,Z. (2008) Dynamics of recognition between tRNA and elongation factor Tu. *J. Mol. Biol.*, **377**, 1382–1405.
31. Schrader,J.M., Chapman,S.J. and Uhlenbeck,O.C. (2011) Tuning the affinity of aminoacyl-tRNA to elongation factor tu for optimal decoding. *Proc. Natl Acad. Sci. USA,***108**, 5215–5220.
32. Uhlenbeck,O.C. and Schrader,J.M. (2018) Evolutionary tuning impacts the design of bacterial tRNAs for the incorporation of unnatural amino acids by ribosomes. *Curr. Opin. Chem. Biol.*, **46**, 138–145.
33. Agris,P.F. (2004) Decoding the genome: a modified view. *Nucleic Acids Res.*, **32**, 223–238.
34. Yarian,C., Townsend,H., Czestkowski,W., Sochacka,E., Malkiewicz,A.J., Guenther,R., Miskiewicz,A. and Agris,P.F. (2002) Accurate translation of the genetic code depends on tRNA modified nucleosides. *J. Biol. Chem.*, **277**, 16391–16395.
35. Agris,P.F. (2008) Bringing order to translation: the contributions of transfer RNA anticodon-domain modifications. *EMBO Rep.*, **9**, 629–635.
36. Näsvall,S.J., Chen,P. and Björk,G.R. (2007) The wobble hypothesis revisited: uridine-5-oxyacetic acid is critical for reading of G-ending codons. *RNA*, **13**, 2151–2164.
37. Manickam,N., Joshi,K., Bhatt,M.J. and Farabaugh,P.J. (2015) Effects of tRNA modification on translational accuracy depend on intrinsic codon–anticodon strength. *Nucleic Acids Res.*, **44**, 1871–1881.
38. Rozov,A., Demeshkina,N., Khusainov,I., Westhof,E., Yusupov,M. and Yusupova,G. (2016) Novel base-pairing interactions at the tRNA wobble position crucial for accurate reading of the genetic code. *Nat. Commun.*, **7**, 10457.
39. Rodriguez-Hernandez,A., Spears,J.L., Gaston,K.W., Limbach,P.A., Gamper,H., Hou,Y.M., Kaiser,R., Agris,P.F. and Perona,J.J. (2013) Structural and mechanistic basis for enhanced translational efficiency by 2-thiouridine at the tRNA anticodon wobble position. *J. Mol. Biol.*, **425**, 3888–3906.
40. Giegé,R., Sissler,M. and Florentz,C. (1998) Universal rules and idiosyncratic features in tRNA identity. *Nucleic Acids Res.*, **26**, 5017–5035.
41. Tamura,K., Himeno,H., Asahara,H., Hasegawa,T. and Shimizu,M. (1992) *In vitro* study of *E. coli* tRNA(Arg) and tRNA(Lys) identity elements. *Nucleic Acids Res.,***20**, 2335–2339.
42. Hibi,K., Amikura,K., Sugiura,N., Masuda,K., Ohno,S., Yokogawa,T., Ueda,T. and Shimizu,Y. (2020) Reconstituted cell-free protein synthesis using in vitro transcribed tRNAs. *Commun. Biol.*, **3**, 350.
43. Miyauchi,K., Ohara,T. and Suzuki,T. (2007) Automated parallel isolation of multiple species of non-coding RNAs by the reciprocal circulating chromatography method. *Nucleic Acids Res.*, **35**, 2–11.

44. Kazayama,A., Yamagami,R., Yokogawa,T. and Hori,H. (2015) Improved solid-phase DNA probe method for tRNA purification: large-scale preparation and alteration of DNA fixation. *J. Biochem*., **157**, 411–418.
45. Tsurui,H., Kumazawa,Y., Sanokawa,R., Watanabe,Y., Kuroda,T., Wada,A., Watanabe,K. and Shirai,T. (1994) Batchwise purification of specific tRNAs by a solid-phase DNA probe. *Anal. Biochem.*, **221**, 166–172.
46. Dong,H., Nilsson,L. and Kurland,C.G. (1996) Co-variation of tRNA abundance and codon usage in *Escherichia coli* at different growth rates. *J. Mol. Biol*, **260**, 649–663.
47. Hartman,M.C.T., Josephson,K. and Szostak,J.W. (2006) Enzymatic aminoacylation of tRNA with unnatural amino acids. *Proc. Natl Acad. Sci. USA*, **103**, 4356–4361.
48. Ma,Zhong and Hartman,MatthewCT (2012) In vitro selection of unnatural cyclic peptide libraries via mRNA display. *Methods Mol. Biol.*, **805**, 367–390.
49. Hartman,M.C.T, Josephson,K., Lin,C.-W. and Szostak,J.W. (2007) An expanded set of amino acid analogs for the ribosomal translation of unnatural peptides. *PLoS One*, **2**, e972
50. Subtelny,A.O., Hartman,M.C.T. and Szostak,J.W. (2011) Optimal codon choice can improve the efficiency and fidelity of N-methyl amino acid Incorporation into peptides by in-vitro translation. *Angew. Chem. Int. Ed.*, **123**, 3222–3225.
51. Buvoli,A., Buvoli,M. and Leinwand,L.A. (2000) Enhanced detection of tRNA isoacceptors by combinatorial oligonucleotide hybridization. *RNA*, **6**, 912–918.
52. Kumazawa,Y., Yokogawa,T., Tsurui,H., Miura,K. and Watanabe,K. (1992) Effect of the higher-order structure of tRNAs on the stability of hybrids with oligodeoxyribonucleotides: separation of tRNA by an efficient solution hybridization. *Nucleic Acids Res.*, **20**, 2223–2232.
53. Reuter,J.S. and Mathews,D.H.(2010) RNAstructure: software for RNA secondary structure prediction and analysis. *BMC Bioinf.*, **11**, 129.
54. Jühling,F., Mörl,M., Hartmann,R.K., Sprinzl,M., Stadler,P.F. and Pütz,J. (2009) tRNAb: compilation of tRNA sequences and tRNA genes. *Nucleic Acids Res.*, **37**, 159–162.
55. Watson,C.N., Belli,A. and Di Pietro,V. (2019) Small non-coding RNAs: new class of biomarkers and potential therapeutic targets in neurodegenerative disease. *Front. Genet.*, **10**, 364.
56. Palazzo,A.F. and Lee,E.S. (2015) Non-coding RNA: what is functional and what is junk?*Front. Genet.*, **6**, 2.
57. Stuart,J.W., Koshlap,K.M., Guenther,R. and Agris,P.F. (2003) Naturally-occurring modification restricts the anticodon domain conformational space of tRNAPhe. *J. Mol. Biol.*, **334**, 901–918.
58. Näsvall,S.J., Chen,P. and Björk,G.R.(2007) The wobble hypothesis revisited: uridine-5-oxyacetic acid is critical for reading of G-ending codons. *RNA*, **13**, 2151–2164.
59. Masuda,I., Hwang,J.-Y., Christian,T., Maharjan,S., Mohammad, Gamper,H., Buskirk,A.R. and Hou,Y.-M. (2021) Loss of N1-methylation of G37 in tRNA induces ribosome stalling and reprograms gene expression. *Elife*, **10**, e70619.
60. Jack,C.-.H., Liu,M. and Horowitz,J. (1998) Recognition of the universally conserved 3′*j*-CCA end of tRNA by elongation factor EF-Tu. *RNA*, **4**, 639–646.
61. Iwane,Y., Kimura,H., Katoh,T. and Suga,H. (2021) Uniform affinity-tuning of N-methyl-aminoacyl-tRNAs to EF-Tu enhances their multiple incorporation. *Nucleic Acids Res.*, **49** , 10807–10817.
62. Iqbal,E.S., Dods,K.K. and Hartman,M.C.T. (2018) Ribosomal incorporation of backbone modified amino acids via an editing-deficient aminoacyl-tRNA synthetase. *Org. Biomol. Chem.*, **16**, 1073–1078.
63. Boccaletto,P., Stefaniak,F., Ray,A., Cappannini,A., Mukherjee,S., Purta,E., Kurkowska,M, Shirvanizadeh,N., Destefanis,E., Groza,P. *et al.* (2022) MODOMICS: a database of RNA modification pathways. 2021 update. *Nucleic Acids Res.*, **50**, D231–D235.